



OPEN ACCESS

EDITED BY

Zhiyuan Hu,
Sun Yat-sen University, China

REVIEWED BY

Xiao Lu,
Sun Yat-sen University, China
Zhenzhong Zeng,
Southern University of Science and
Technology, China

*CORRESPONDENCE

Xu Yue,
✉ yuexu@nuist.edu.cn

RECEIVED 10 August 2023

ACCEPTED 12 October 2023

PUBLISHED 25 October 2023

CITATION

Hu Y, Yue X, Tian C, Zhou H, Fu W, Zhao X,
Zhao Y and Chen Y (2023), Identifying the
main drivers of the spatiotemporal
variations in wetland methane emissions
during 2001–2020.
Front. Environ. Sci. 11:1275742.
doi: 10.3389/fenvs.2023.1275742

COPYRIGHT

© 2023 Hu, Yue, Tian, Zhou, Fu, Zhao,
Zhao and Chen. This is an open-access
article distributed under the terms of the
[Creative Commons Attribution License
\(CC BY\)](https://creativecommons.org/licenses/by/4.0/). The use, distribution or
reproduction in other forums is
permitted, provided the original author(s)
and the copyright owner(s) are credited
and that the original publication in this
journal is cited, in accordance with
accepted academic practice. No use,
distribution or reproduction is permitted
which does not comply with these terms.

Identifying the main drivers of the spatiotemporal variations in wetland methane emissions during 2001–2020

Yihan Hu¹, Xu Yue^{1*}, Chenguang Tian¹, Hao Zhou², Weijie Fu¹,
Xu Zhao¹, Yuan Zhao¹ and Yuwen Chen¹

¹School of Environmental Science and Engineering, Nanjing University of Information Science and Technology (NUIST), Nanjing, China, ²Climate Change Research Center, Institute of Atmospheric Physics, Chinese Academy of Sciences, Beijing, China

Wetlands act as an important natural source of global methane (CH₄). The emission rate of wetland CH₄ is jointly affected by climate change, carbon dioxide (CO₂) fertilization, and wetland distribution. In this study, we implemented a wetland CH₄ emission module into the Yale Interactive Biosphere (YIBs) model to quantify the spatiotemporal variations of global wetland CH₄ emissions in 2001–2020. Site-level validations showed that the YIBs model reasonably captures the seasonality and magnitude of CH₄ emissions at 28 out of 33 sites with significantly positive correlations and low relative biases. On the global scale, the YIBs predicts an annual mean wetland CH₄ emission of 147.5 Tg yr⁻¹ in 2000–2017, very close to the estimate of 147.9 Tg yr⁻¹ from the ensemble of 13 process-based models. Global wetland CH₄ emissions showed a positive trend of 0.74 Tg yr⁻² in the past 2 decades, leading to an increase of 7.4 Tg yr⁻¹ (5.2%) in 2008–2017 than 2000–2009. Climate change and CO₂ fertilization accounted for over 70% of global wetland CH₄ emission changes. Among them, the impact of CO₂ grew steadily and became the dominant factor after the year 2008. The most significant changes in wetland CH₄ emissions were located in the tropical regions following the perturbations in temperature that drives the ecosystem productivity. We found limited changes in CH₄ emissions over high latitudes because of the moderate variations in wetland area fraction. The rise of wetland CH₄ emissions poses an emerging threat to the global warming and likely escalates the tropospheric air pollutants.

KEYWORDS

wetland, methane, climate change, CO₂ fertilization, YIBs model

1 Introduction

Atmospheric methane (CH₄) is an important greenhouse gas (Fletcher and Schaefer, 2019) and precursor of tropospheric ozone (Staniaszek et al., 2022). The CH₄ concentrations have been steadily increasing since the preindustrial period (Aben et al., 2017). Recent observations showed a CH₄ rise of 267 ppb (16.2%) from 1984 to 2022 though with large interannual variations (Lan et al., 2022). Such increase of CH₄ is mainly driven by the changes of emissions, especially from the anthropogenic sources that grew 26% during 1970–2012 (Turner et al., 2019). However, the natural emissions of CH₄ also account for

approximately 28% of the global CH₄ emissions and made important contributions to the growth of atmospheric CH₄ levels (Saunois et al., 2020).

The wetland CH₄ emission is the largest component of natural sources (Koffi et al., 2020). Production of wetland CH₄ involves complex biogeochemical processes and is highly sensitive to climatic and environmental perturbations. High temperature promotes CH₄ emissions with a Q₁₀ metric and further escalates emissions with a warming feedback (Liu et al., 2020; Rößger et al., 2022; Zhang et al., 2023). Precipitation usually increases wetland emissions by enlarging the area of waterbody and increasing the water table depth (Lunt et al., 2021; Zou et al., 2022), the latter of which may further increase the temperature sensitivity of CH₄ emissions (Duval and Radu, 2018; Chen et al., 2021). The variation of wetland area caused by the shifts in precipitation and temperature patterns directly determine the area of wetland methane discharge (Kuhn et al., 2018; Zou et al., 2022). Increased CO₂ concentration can lead to an increase in microbial biomass of methanogens by promoting the ecosystem productivity and the mineralization of soil organic matter (Liu et al., 2019; Yuan et al., 2021). The changes of these environmental factors modulate the spatiotemporal variations in the regional to global wetland CH₄ emissions.

Different approaches have been applied to estimate global wetland CH₄ emissions, including the top-down estimates of 155.5–218.6 Tg yr⁻¹ using the inverse modeling and satellite-based observations (Ishizawa et al., 2016; Bergamaschi et al., 2018), as well as the bottom-up estimates of 100.1–183.2 Tg yr⁻¹ with process-based models and site-level measurements (Zhu et al., 2015; Arora et al., 2018). Among these methods, the process-based models show advantages in predicting historical emissions and identifying the dominant drivers. Most models consider the biogeochemical processes such as production, oxidation, and transport for CH₄ emissions (Wania et al., 2010; Nzotungicimpaye et al., 2021; Salmon et al., 2022). For example, the LPJ-WHyMe model reasonably captures the seasonal variations of CH₄ emissions at seven sites by adding a root exudate pool with stratified root distribution to the major biogeochemical processes (Wania et al., 2010). The WETMETH model also considers the above processes with dynamic predictions of soil water table and inundation areas, and shows consistent spatial patterns with three upscaled flux measurements (Nzotungicimpaye et al., 2021). The ORCHIDEE model with the permafrost dynamics and optimized parameters can reasonably simulate methane emissions from the northern wetlands (Salmon et al., 2022).

In addition to the above-mentioned individual simulations, the recent estimates with 13 models predicted natural wetland CH₄ emissions of 101–179 Tg yr⁻¹ on the global scale during 2000–2017 (Saunois et al., 2020). These models were driven with the same meteorology and boundary conditions, so as to minimize the modeling uncertainties due to the forcing data. However, they prescribed the wetland net primary productivity (NPP) and ignored the CO₂ fertilization effects to the changes in substrate availability. As a result, the multi-model ensemble average suggests a very limited trend in wetland CH₄ emissions for 2000–2017 (Saunois et al., 2020), which are inconsistent with the fast growth of atmospheric CH₄ levels (Lan et al., 2022) and the recent increase of wetland emissions

(Shaw et al., 2022). Furthermore, the drivers of the changes in wetland CH₄ emissions were not explored.

In this study, we implemented a process-based wetland CH₄ emissions scheme into the well-established Yale Interactive terrestrial Biosphere (YIBs) model (Yue and Unger, 2015). We evaluate the simulated wetland emissions against *in situ* measurements and the multi-model ensemble averages. The model is then driven with year-to-year CO₂ concentrations, meteorological parameters, and wetland extent to predict global wetland CH₄ emissions during 2000–2020. We perform sensitivity experiments to quantify the contributions of individual factors to the trends in CH₄ emissions. With these model configurations, we attempt to depict the spatiotemporal variations of wetland CH₄ emissions and identify their dominant drivers in the past two decades.

2 Methods and data

2.1 YIBs vegetation model

We use the YIBs model as the framework for wetland CH₄ emissions. The YIBs is a vegetation model that simulates carbon fluxes with prognostic leaf area index (LAI) and tree height (Yue and Unger, 2015). The model applies the Michaelis-Menten enzyme-kinetics scheme for leaf photosynthesis (Farquhar et al., 1980) and the two-leaf canopy radiative transfer scheme for light partitioning (Spitters et al., 1986). The gross primary productivity (GPP) is calculated by the integration of leaf photosynthesis along the LAI. The litterfall drives the carbon transitions among soil pools and the heterotrophic respiration (R_h). The accumulation of soil carbon provides substrate for the wetland CH₄ emissions. Simulated GPP and LAI have been validated against site-level and satellite-based observations (Yue et al., 2015). The YIBs model has joined the vegetation model intercomparison project since 2020 and showed reasonable performance in the simulation of major carbon metrics including GPP, LAI, vegetation biomass, soil carbon and so on (Friedlingstein et al., 2020).

2.2 Wetland CH₄ emission module

We implement a process-based wetland CH₄ emission module into the YIBs with major biogeochemical processes, including production, oxidation, and transportation of CH₄. In the wetland areas, the production of CH₄ is calculated based on soil conditions (including soil temperature and pH) and the amount of carbon that is distributed for methanation, following the CH₄-related module in the TRIPLEX-GHG model (Zhu et al., 2014). The decomposition of organic matter is regulated by redox acceptors. Under anaerobic conditions, the presence of high organic substrates restricts the redox potential, controlling the decomposition rate of organic carbon and the emissions ratio of CH₄ and carbon dioxide. The R_h during anaerobic decomposition processes is derived as the remaining portion after subtracting net ecosystem productivity (NEP) from net primary productivity (NPP). The rate of CH₄ oxidation is computed using a Michaelis-Menten kinetic relationship that is dependent on temperature and CH₄

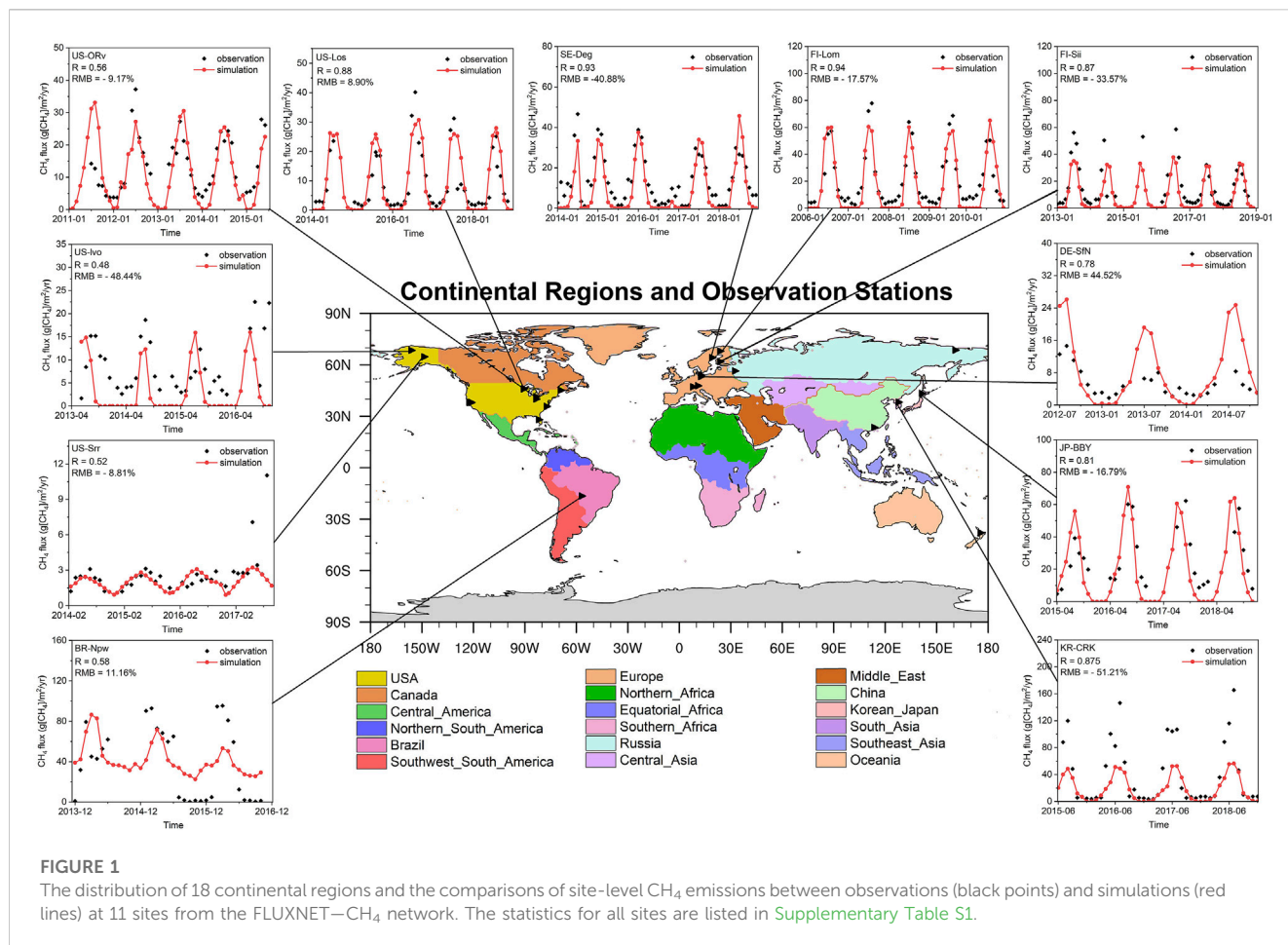


FIGURE 1 The distribution of 18 continental regions and the comparisons of site-level CH₄ emissions between observations (black points) and simulations (red lines) at 11 sites from the FLUXNET–CH₄ network. The statistics for all sites are listed in [Supplementary Table S1](#).

concentrations in the corresponding soil layer (Dunfield et al., 1993). The transportation of CH₄ from soil to atmosphere is composed of three pathways including diffusion, ebullition, and plant-mediated transportation. The diffusion of CH₄ follows the Fick’s law with the dependence on soil properties (soil texture, tortuosity and water content) and CH₄ concentration gradient between different soil layers (Walter and Heimann, 2000). The ebullition of CH₄ is triggered if the CH₄ concentration exceeds 750 μmol L⁻¹ (Zhu et al., 2014). The plant-mediated transportation, which provides an impactful way to divert CH₄ from soil to atmosphere, is calculated based on the same aerenchyma factor of plants as those equations used in the TRIPLEX-GHG model (Zhu et al., 2014).

2.3 Data for simulations and validations

We use the meteorological variables from the MERRA-2 reanalysis (Gelaro et al., 2017) to drive the YIBs model. The surface variables include air temperature, specific humidity, solar radiation, air pressure, and wind speed. The soil variables include soil temperature and soil moisture at six vertical layers. All these variables are interpolated to the horizontal resolution of 1° × 1° at the hourly time step. The year-to-year global mean atmospheric CO₂ concentrations are adopted from the protocol data for the input4MIPs (<https://esgf-node.llnl.gov/projects/input4mips/>).

For the wetland CH₄ scheme, we used the monthly global wetland extent dataset of WAD2M (Zhang Z. et al., 2021) derived from remote sensing and the soil pH map of SoilGrids250m dataset (Hengl et al., 2017) from the International Soil Reference and Information Centre. Other gridded soil parameters (e.g., particle composition, soil porosity) are obtained from the ISLSCP II Global Gridded Soil Characteristics dataset (Scholes et al., 2011) generated by the International Satellite Land-Surface Climatology Project.

We use site-level measurements from the FLUXNET-CH₄ network (Delwiche et al., 2021) to validate the simulated CH₄ emissions. The monthly CH₄ fluxes are collected from all the available 33 sites with at least 3 years length of period. We also use the multi-model output from 13 bottom-up models and 9 top-down approaches to assess the simulated wetland emissions during 2000–2017. To facilitate the comparison, we separate the global land into 18 regions following the definitions in Saunois et al. (2020) (Figure 1).

2.4 Simulations

We perform four simulations to depict the spatiotemporal variations of wetland CH₄ emissions (Table 1). The BASE run is forced with year-to-year meteorology, wetland extent, and CO₂ concentrations during 2000–2020. Three “FIX” sensitivity

TABLE 1 Summary of sensitivity experiments.

Simulations	Climate	Wetland extent	CO ₂ concentration
BASE	2000–2020	2000–2020	2000–2020
FIXCLIM	2000	2000–2020	2000–2020
FIXWET	2000–2020	2000	2000–2020
FIXCO ₂	2000–2020	2000–2020	2000

experiments are conducted to distinguish the impacts of the changes in climate (CLIM), wetland area (WET), and CO₂ fertilization effects (CO₂) on CH₄ emissions. For each of these runs, all the forcings are the same as BASE run except that a specific forcing is fixed at the year 2000. The differences between the BASE and “FIX” runs indicate the contributions of changes in climate (BASE–FIXCLIM), wetland (BASE–FIXWET), and CO₂ (BASE–FIXCO₂) to the global wetland CH₄ emissions. For all simulations, the hourly meteorology is applied from 1900 to 2020 with the cycling of 2000 meteorology for the 1900–2000 period, which is used for the model spin up.

3 Result

3.1 Model evaluations and comparisons

We first evaluate the simulated CH₄ emissions at FLUXNET-CH4 sites (Figure 1). For the selected sites around the world, the YIBs model in general captures the seasonality of CH₄ emissions with the peak values in summer period. Among the total of 33 sites, simulations show significantly positive correlation coefficients (R) at 28 sites and reasonable relative mean biases (RMB) of –50%–50% at 23 sites (Supplementary Table S1). Emissions are usually higher nearby the tropical rainforest but lower in the semi-arid regions such as western United States. For the Amazon rainforest with dense vegetation, the non-flooded trees can absorb CH₄ from the soil through their roots, transport the gas through vascular systems to stems, and release it into the air subsequently (Gauci et al., 2021). The model fails to capture the CH₄ emissions at some sites. For example, simulated CH₄ fluxes are negatively correlated with a high RMB of 186% against measurements at site US-Snd. However, this site is within the same grid as US-Sne and US-Srr where the YIBs model yields reasonable emissions. A similar case could be found at US-Twt, US-Tw1, and US-Tw4 where the simulations share the same values due to the vicinity of sites but observations exhibit large deviations. As a result, the missing of site-specific parameters (such as vegetation types, soil characteristics) may in part cause the modeling biases at these sites.

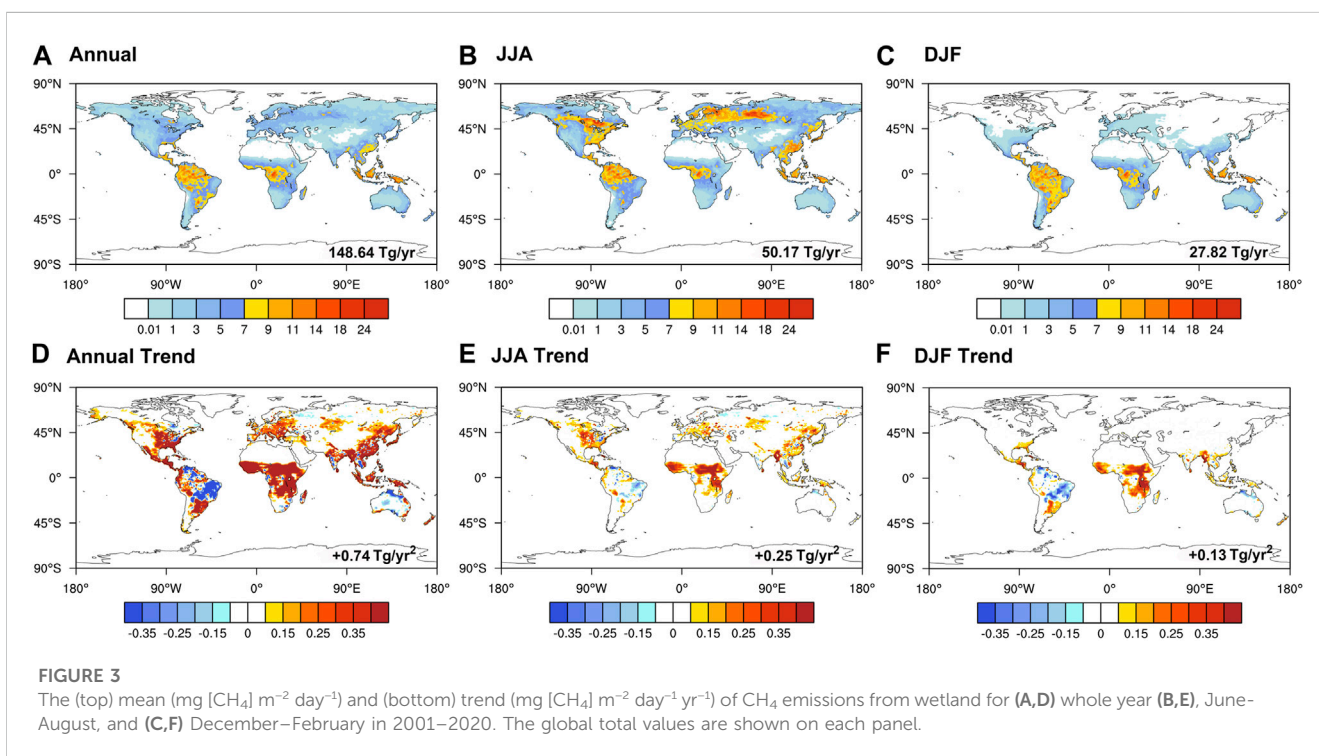
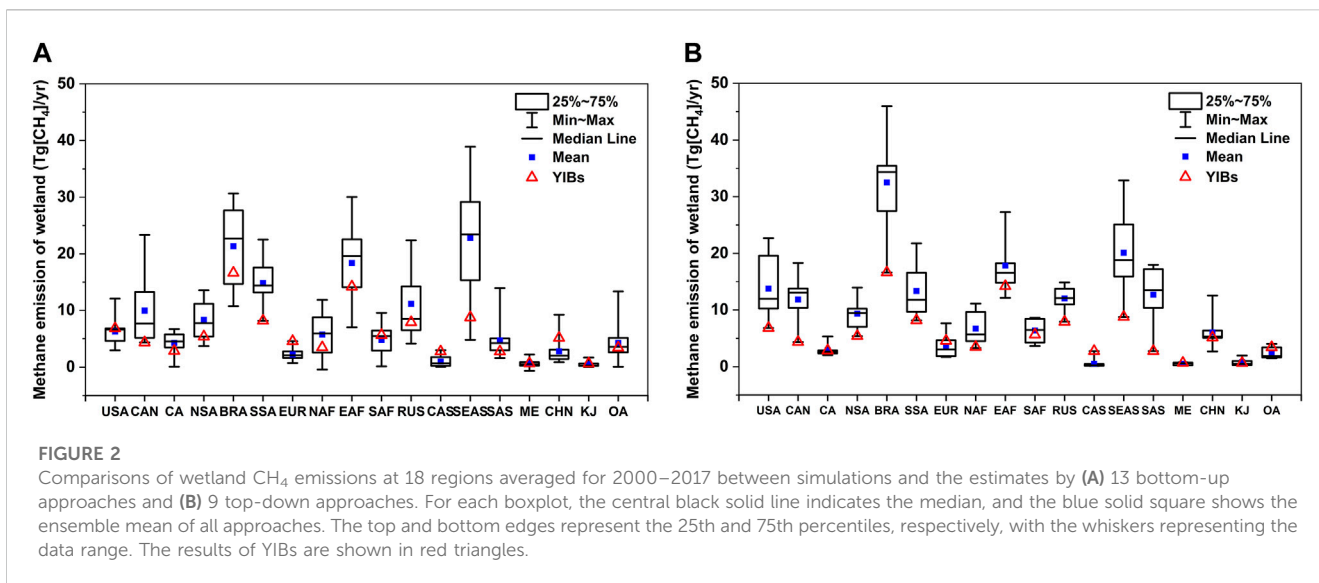
We then compare the simulated global wetland CH₄ emissions with other estimates (Supplementary Table S2). On average, the emissions estimated by process-based models are 19.1% lower than those using the top-down approaches. Compared to the ensemble of 13 bottom-up models, the YIBs shows lower value of –2.1% in 2000–2009 and the higher estimate of 1.6% in 2008–2017. For the ensemble mean of models, limited differences are found between the two periods likely because of the omission of CO₂ fertilization effects

on the wetland NPP (Saunois et al., 2020). However, for individual models, either positive (7 out of 13), negative (2 out of 13), or mild (4 out of 13) trends are predicted because of their varied representations of climatic impacts on CH₄ emissions. A similar conclusion is achieved with the nine top-down approaches utilizing the WAD2M wetland dataset. The maximum increases in CH₄ emissions between the two decades are predicted at 3.6% for the top-down and 5.2% for the bottom-up methods, respectively. The predicted trend of 5.2% with the YIBs model is at the high end of other estimates, though our simulations consider the CO₂ fertilization effect.

We compare the simulated trend of wetland CH₄ emissions with the top-down inversion (Zhang Y. et al., 2021) from the Greenhouse gases Observing Satellite (GOSAT). The growth rate of natural wetland CH₄ in the YIBs model shows increased emissions after the year 2010 (Supplementary Figure S1A). The simulated trend of 12.09% matches that of 12.29% from the posterior data of GOSAT, which shows a much larger interannual variability than the simulations. Such year-to-year variations are difficult to reproduce as the prior data fail to capture both the interannual perturbations and the long-term trend. Furthermore, we compare the simulated interannual variations with the results of LPJ model (Zhang et al., 2023) driven by meteorological fields from either Climatic Research Unit (CRU) or MERRA-2 reanalyses (Supplementary Figure S1B). The growth rates obtained from different meteorological fields exhibit a maximum deviation of up to 11.62%. Using the same meteorological field of MERRA2, the moderate difference of 2.03% is achieved between the simulations of YIBs and LPJ models. Such discrepancy is lower than the differences caused by the varied meteorological fields.

We divide global land into 18 regions (Figure 1) where the simulated wetland CH₄ emissions are compared to the values from multiple models and approaches (Figure 2). Comparing the results from different approaches, the assessment of natural wetland CH₄ emissions by bottom-up models tends to be lower than that of top-down approaches in most regions (Supplementary Figure S2A). Similar to other bottom-up models, the YIBs model yields lower emission estimates in multiple regions compared to the top-down models especially over the Canada, Brazil, and Southeast Asia regions. On average, the simulated CH₄ emissions match the medians of multiple models with a high R² of 0.77, though the former is in general lower than the latter estimates (Supplementary Figure S2B).

In all the 18 regions, YIBs model yields reasonable wetland CH₄ emissions with differences of –15.2 Tg yr^{–1} ~ 2.54 Tg yr^{–1} from the multi-model ensemble medians. For comparison of top-down models and bottom-up models, both methods show the same top two emitters in Brazil and Southeast Asia, though the top-down approach predicts much higher emissions in Brazil than the latter region. The YIBs also yields the largest wetland CH₄ emissions in Brazil, but underestimates the emissions in Southeast Asia by 56.82%–63.37% compared to the multi-model ensemble mean. The median assessments of CH₄ emissions from the third-largest natural wetland region in Africa by bottom-up models, top-down approaches, and YIBs model are relatively close, ranging from 14.21 to 18.72 Tg yr^{–1}. However, there is a relatively significant divergence among different models in the assessments over high-emission regions, like Brazil, Southeast Asia and Equatorial Africa.



We also found large inter-model variability in Canada and Russia though the emissions are much lower than the tropical region, which is likely associated with the varied sensitivity to climatic drivers among different models and approaches (Saunois et al., 2020). In most regions, the performance of the YIBs model is relatively close to the intermediate levels of other bottom-up models. However, it yields significantly higher assessment of emissions in Central Asia compared to most models, though it does not exceed the maximum values among the other 13 bottom-up models. The discrepancies underscore the substantial uncertainty in the current assessment of natural wetland CH₄ emissions, primarily attributed to the complex biogeochemical

and ecological processes involved in the processes. The variations among models in different processes may further magnify the differences in the final emission estimates. In future researches, more observations are required to validate the simulated CH₄ emissions from natural wetlands in different regions.

3.2 Spatiotemporal variation in wetland CH₄ emissions

The wetland CH₄ emissions show distinct spatial and seasonal variations (Figure 3). Large emissions are located in the tropics

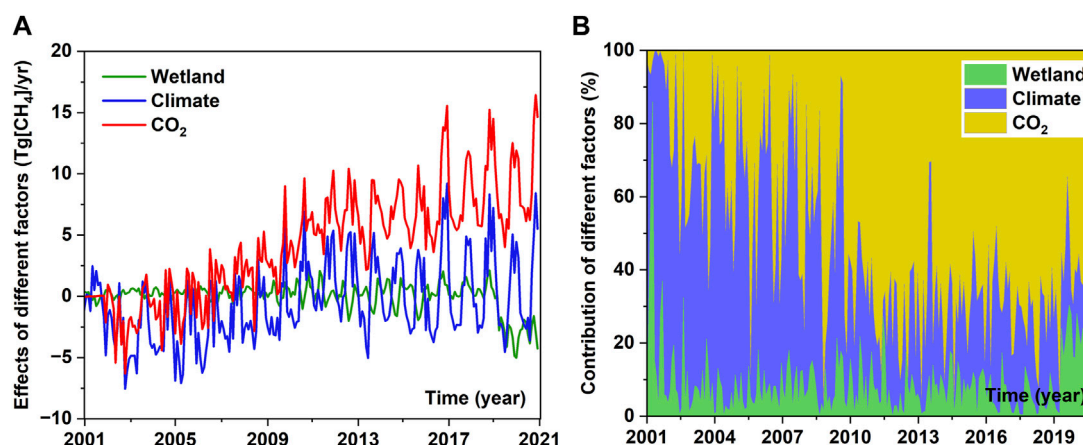


FIGURE 4

The (A) variations of wetland CH₄ emissions and (B) contributions of three key driving factors including wetland extent, climate change, and CO₂ fertilization during 2001–2020. The contribution percentages for individual factors are derived based on the absolute changes from baseline simulation caused by prescribing the specific factor.

(23.5°S–23.5°N), contributing 69.22% to the global total amount due to the optimal hydrothermal conditions and the adequate supply of substrate. The secondary hotspots are found in the temperate (23.5°N–60°N) regions of the Northern Hemisphere, which accounts for 24.32% of the global amount (Figure 3A). These centers become the strongest in the boreal summer (Figure 3B), when the high temperature promotes CH₄ emission rate and expand the wetland extent. The total global emissions in summer (from June to August) reach 50.2 Tg, accounting for 33.8% of the annual total amount. In contrast, limited emissions are predicted over the northern mid-high latitudes in boreal winter because of the low temperature and seasonally frozen ground. For this season, most of global wetland CH₄ emissions are confined in the tropical regions, leading to 45% lower emissions compared to the summertime on the global scale.

We further assess the trend of wetland CH₄ emissions during 2001–2020. Over the global grids with baseline emissions of at least 1 mg m⁻² day⁻¹, 1.47% show significant increase in the past two decades. The most significant enhancement is located at the tropical Africa, eastern Asia, and eastern United States. (Figure 3D). The increase of CH₄ emissions in tropical Africa persist all year round, while those in Asia and US are more evident in boreal summer (Figures 3E, F). Meanwhile, large reduction is predicted over eastern South America, where the baseline emissions (Figure 3A) are low due to the moderate supply of substrate from grassland. Such regional decline is more evident in boreal winter (Figure 3F). On the global scale, the positive trend in summer almost doubles that in winter.

3.3 Drivers of the trends in wetland CH₄ emissions

We isolate the contributions of climate change, CO₂ fertilization, and wetland extent to the trend of CH₄ emissions during 2001–2020 (Figure 4). Among these factors, the changes

of wetland area show limited impacts while the other two factors cause large variabilities in CH₄ emissions (Figure 4A). For 2001–2008, the negative effects of climate change play the dominant role in regulating the total trend. However, after the year 2008, the impact of CO₂ fertilization is becoming more important year by year, accounting for 67.84% of the total changes in CH₄ emissions during 2010–2020 (Figure 4B). For the FIXCO₂ simulation, the average wetland CH₄ emissions are predicted to be 143.47 Tg yr⁻¹ in 2000–2009 and 143.26 Tg yr⁻¹ in 2008–2017. As a result, the YIBs model yields limited changes in wetland CH₄ emissions between the 2 decades, close to the estimate by the ensemble of 13 process-based models without the CO₂ fertilization effects (Supplementary Table S2).

We further identify the spatial distribution of wetland CH₄ changes induced by different factors (Figure 5). Climate change alone exerts strong impacts in tropical regions with CH₄ reductions in South America, South Africa, and Australia, but increased emissions in central Africa (Figure 5A). There are some moderately positive changes in CH₄ emissions induced by climate at the middle latitudes of Northern Hemisphere. The positive and negative changes are offsetting each other, leading to a limited contribution of -0.12 Tg yr⁻¹ by climate change during 2001–2020. CO₂ fertilization causes widespread enhancement in CH₄ emissions especially over the tropical regions (Figure 5B). The changes in wetland area cause patchy responses in CH₄ emissions with moderate reductions in South America and central Africa (Figure 5C).

In anaerobic environments, the rate of organic carbon decomposition and the release ratio of carbon dioxide to methane are constrained by the presence of high organic matter substrates. Climate change decreases R_h in South America, South Africa, and Australia (Figure 6A), because increased temperature (Figure 6C) inhibits plant photosynthesis in the tropical regions (Piao et al., 2013). In contrast, the slight cooling over Sahel and central Africa promotes the regional R_h (Figure 6A) and the consequent

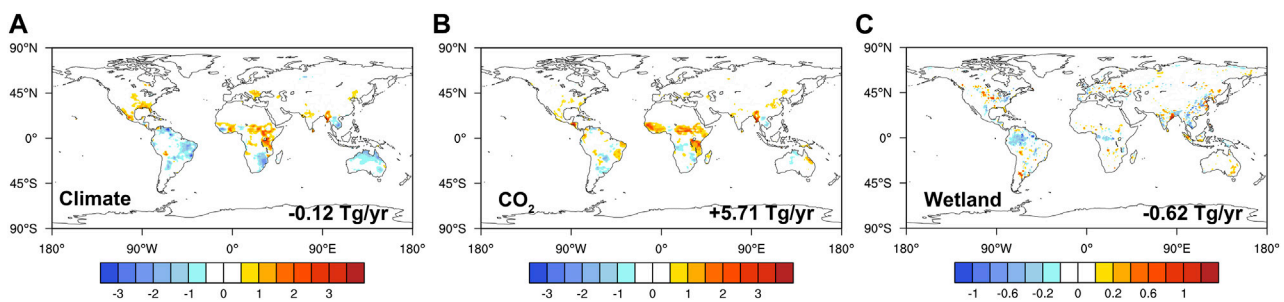


FIGURE 5

The mean differences in wetland CH_4 emissions (Units: $\text{mg}[\text{CH}_4] \text{ m}^{-2} \text{ day}^{-1}$) between simulations with all forcing (BASE) and that with fixed (A) climate (FIXCLIM), (B) CO_2 (FIX CO_2) and (C) wetland extent (FIXWET) during 2001–2020.

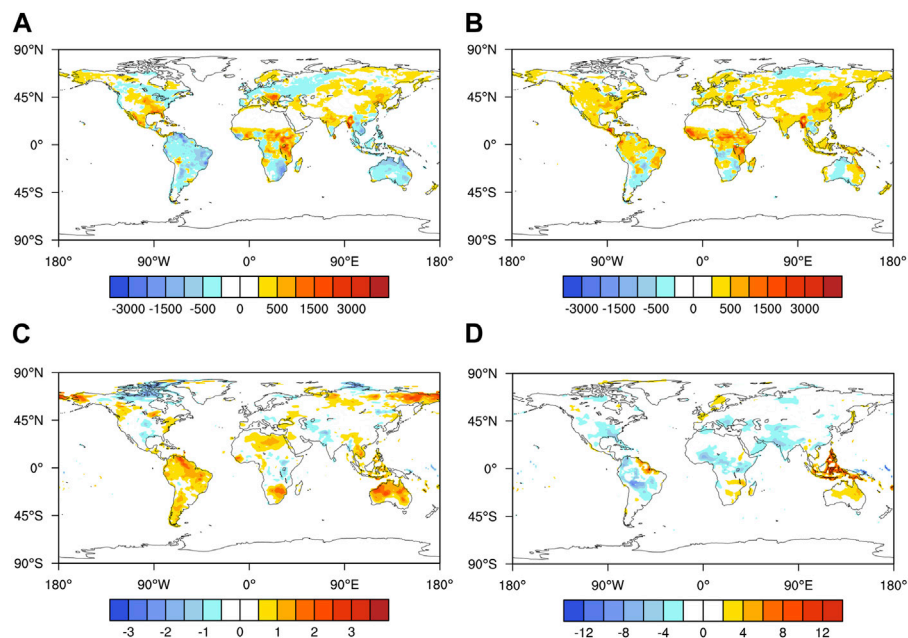


FIGURE 6

The trend of heterotrophic respiration (Units: $\text{mg}[\text{C}] \text{ m}^{-2} \text{ day}^{-1}$) induced by (A) climate change and (B) CO_2 fertilization, as well as the trend in (C) temperature (Units: $^{\circ}\text{C}$) and (D) solar radiation (Units: W m^{-2}) during 2001–2020.

wetland CH_4 emissions (Figure 5A). Solar radiation shows widespread reductions except over Indonesia and Australia (Figure 6D). However, the effect of radiation change on R_h is secondary to that of temperature, as the warming-induced inhibition outweighs the benefit of increased radiation in Indonesia and Australia (Figure 6A). The CO_2 fertilization effect causes increases in R_h globally (Figure 6B), leading to significant enhancement of wetland CH_4 emissions. (Figure 5B).

4 Conclusion and discussion

We implemented a wetland CH_4 emission module into the YIBs vegetation model and validated its performance against

available measurements and estimates. Simulated wetland CH_4 emissions matched observations with reasonable seasonality at 28 out of 33 sites. The model also yielded similar global wetland CH_4 emissions compared to the ensemble of 13 process-based models. We performed sensitivity experiments to identify the spatiotemporal variations of wetland CH_4 emissions and the associated drivers from 2001 to 2020. The results showed that the interannual variation of atmospheric CO_2 and meteorological conditions predominantly drive the changes in global wetland CH_4 emissions, with their combined contributions exceeding 70% in each month during the research period. The role of CO_2 fertilization grew gradually and became the dominant factor after 2008. The attribution analyses indicated that the changes of wetland CH_4 emissions followed the changes in R_h ,

with widespread enhancement by CO₂ fertilization effects but patchy responses to climate change mainly following the trend of temperature.

Previous studies also revealed the strong impacts of CO₂ fertilization on wetland CH₄ emissions. For example, [Yuan et al. \(2021\)](#) suggested that increased CO₂ could promote the concentration of dissolved organic carbon (DOC) and acetate by enhancing ecosystem productivity and the mineralization of soil organic matter. This, in turn, leads to an increase in the microbial biomass of methanogens, ultimately resulting in enhanced CH₄ emissions. However, some recent estimates ignored the CO₂ fertilization effect in their simulations. For example, the observation-constrained study by [Koffi et al. \(2020\)](#) showed enhanced wetland CH₄ emissions of 50%–80% at the end of 21st century without considering CO₂ fertilization effect. The multi-model ensemble estimates by [Saunois et al. \(2020\)](#) also neglected the CO₂ fertilization and achieved limited trends in wetland CH₄ emissions for the recent two decades. We expect that the increasing rates of wetland CH₄ emissions are likely underestimated in above studies as the role of CO₂ fertilization becomes more dominant over the long-term period.

Many studies have emphasized the influences of climatic factors on wetland CH₄ emissions. [Liu et al. \(2020\)](#) highlighted the important role of air temperature, which affects CH₄ production directly through Q₁₀ factors and indirectly by altering both NPP and wetland inundation area fraction. We also found that temperature accounts for most of climate-driven changes in CH₄ emissions through modulating ecosystem NPP ([Figure 6](#)). Furthermore, [Chen et al. \(2021\)](#) observed a positive correlation between wetland water level and temperature sensitivity in CH₄ emissions, though this relationship is not incorporated in our model. [Zhang et al. \(2023\)](#) compared the impacts of temperature and precipitation, and found that precipitation dominates the variability of CH₄ emissions in some tropical regions as rainfall alter the wetland extent. However, we prescribed the area of wetland in our simulations and constrained the effects of precipitation to some extent. Despite these discrepancies, we also found that the perturbations of tropical CH₄ dominates the global wetland emissions as concluded by [Zhang et al. \(2023\)](#).

In this study, we found limited changes of wetland CH₄ emissions at high latitudes. The melting permafrost in boreal regions of the Northern Hemisphere is expected to become a crucial source in the future, as projected by the Coupled Model Intercomparison Project ([Canadell et al., 2021](#)). However, there is considerable disagreement regarding the assessment of the impact of permafrost melting on CH₄ emissions. [Zhang et al. \(2017\)](#) estimated that CH₄ emissions could reach 347.8 Tg yr⁻¹ by the end of the 21st century under the RCP8.5 scenario taking into account the wetland expansion from permafrost melting. Nonetheless, the inversion-constrained estimation showed much lower CH₄ emissions under the same climate change scenario ([Koffi et al., 2020](#)). Furthermore, [Salmon et al. \(2022\)](#) found that bottom-up models tend to overestimate CH₄ emissions in northern peatland sites in the model calibrations. These studies revealed the large uncertainties in estimating wetland CH₄ emissions due to the permafrost dynamics in

process-based models. It should be noted that global wetland area distributions derived from satellite retrievals may also deviate from the actual conditions. The retrievals are influenced by the accuracy of prior data ([Xi et al., 2022](#)) and it is challenging to adequately validate retrieval results in regions lacking ground-based observations. Additionally, the low surface reflectance features such as limestone deposits may lead to overestimations of inundation levels in certain areas ([Jensen and McDonald, 2019](#)). Non-wetland areas in dynamic dataset with an inundation index of 0 do not necessarily imply the absence of wetlands. These limitations of the wetland area dataset may introduce uncertainties into our assessment of the global variations in wetland CH₄ emissions. Despite these uncertainties, we revealed an increasing tendency of wetland CH₄ emissions due to the joint effects of CO₂ fertilization and climate change in the past two decades. Such trend likely persists under global warming and poses an emerging threat to both climate and air quality.

Data availability statement

The original contributions presented in the study are included in the article/[Supplementary Material](#), further inquiries can be directed to the corresponding author.

Author contributions

YH: Conceptualization, Data curation, Methodology, Writing–original draft, Writing–review and editing. XY: Conceptualization, Data curation, Methodology, Writing–original draft, Writing–review and editing, Funding acquisition. CT: Data curation, Investigation, Writing–review and editing. HZ: Data curation, Investigation, Writing–review and editing. WF: Data curation, Investigation, Writing–review and editing. XZ: Data curation, Investigation, Writing–review and editing. YZ: Data curation, Investigation, Writing–review and editing. YC: Data curation, Investigation, Writing–review and editing.

Funding

The authors declare financial support was received for the research, authorship, and/or publication of this article. This study was jointly supported by the National Natural Science Foundation of China (grant no. 42293323) and Natural Science Foundation of Jiangsu Province (grant no. BK20220031).

Acknowledgments

The authors thank the NASA for the MERRA-2 reanalysis datasets and ISLSCP II Global Gridded Soil Characteristics dataset, the ISRIC for SoilGrids 250m datasets, the ESGF for input4MIPs, the FLUXNET-CH4 community for methane observation data, and Zhang et al. for WAD2M dataset.

Conflict of interest

The authors declare that the research was conducted in the absence of any commercial or financial relationships that could be construed as a potential conflict of interest.

Publisher's note

All claims expressed in this article are solely those of the authors and do not necessarily represent those of their affiliated

organizations, or those of the publisher, the editors and the reviewers. Any product that may be evaluated in this article, or claim that may be made by its manufacturer, is not guaranteed or endorsed by the publisher.

Supplementary material

The Supplementary Material for this article can be found online at: <https://www.frontiersin.org/articles/10.3389/fenvs.2023.1275742/full#supplementary-material>

References

- Aben, R., Barros, N., Donk, E., Frenken, T., Hilt, S., Kazanjian, G., et al. (2017). Cross continental increase in methane ebullition under climate change. *Nat. Commun.* 8, 1682. doi:10.1038/s41467-017-01535-y
- Arora, V. K., Melton, J. R., and Plummer, D. (2018). An assessment of natural methane fluxes simulated by the CLASS-CTEM model. *Biogeosciences* 15, 4683–4709. doi:10.5194/bg-15-4683-2018
- Bergamaschi, P., Karstens, U., Manning, A. J., Saunio, M., Tsuruta, A., Berchet, A., et al. (2018). Inverse modelling of European CH₄ emissions during 2006–2012 using different inverse models and reassessed atmospheric observations. *Atmos. Chem. Phys.* 18, 901–920. doi:10.5194/acp-18-901-2018
- Canadell, J. G., Scheel Monteiro, P., Costa, M. H., Cotrim da Cunha, L., Cox, P. M., Eliseev, A. V., et al. (2021). “Global carbon and other biogeochemical cycles and feedbacks,” in *Climate change 2021: the physical science basis. Contribution of working group I to the sixth assessment report of the intergovernmental panel on climate change*. V. Masson-Delmotte, P. Zhai, A. Pirani, S. L. Connors, C. Péan, S. Berger, et al. (Cambridge, United Kingdom and New York, NY, USA: Cambridge University Press), 673–816. doi:10.1017/9781009157896.001
- Chen, H., Xu, X., Fang, C., Li, B., and Nie, M. (2021). Differences in the temperature dependence of wetland CO₂ and CH₄ emissions vary with water table depth. *Nat. Clim. Change* 11, 766–771. doi:10.1038/s41558-021-01108-4
- Delwiche, K. B., Knox, S. H., Malhotra, A., Fluet-Chouinard, E., McNicol, G., Feron, S., et al. (2021). FLUXNET-CH₄: a global, multi-ecosystem dataset and analysis of methane seasonality from freshwater wetlands. *Earth Syst. Sci. Data* 13, 3607–3689. doi:10.5194/essd-13-3607-2021
- Dunfield, P., Knowles, R., Dumont, R., and Moore, T. R. (1993). Methane production and consumption in temperate and subarctic peat soils: response to temperature and pH. *Soil Biol. Biochem.* 25, 321–326. doi:10.1016/0038-0717(93)90130-4
- Duval, T. P., and Radu, D. D. (2018). Effect of temperature and soil organic matter quality on greenhouse-gas production from temperate poor and rich fen soils. *Ecol. Eng.* 114, 66–75. doi:10.1016/j.ecoleng.2017.05.011
- Farquhar, G. D., Von Caemmerer, S., and Berry, J. A. (1980). A biochemical model of photosynthetic CO₂ assimilation in leaves of C₃ species. *Planta* 149, 78–90. doi:10.1007/BF00386231
- Fletcher, S. E. M., and Schaefer, H. (2019). Rising methane: a new climate challenge. *Science* 364, 932–933. doi:10.1126/science.aaxi828
- Friedlingstein, P., O'Sullivan, M., Jones, M. W., Andrew, R. M., Hauck, J., Olsen, A., et al. (2020). Global carbon budget 2020. *Earth Syst. Sci. Data* 12, 3269–3340. doi:10.5194/essd-12-3269-2020
- Gauci, V., Figueiredo, V., Gedney, N., Pangala, S. R., Stauffer, T., Weedon, G. P., et al. (2021). Non-flooded riparian Amazon trees are a regionally significant methane source. *Philos. Trans. R. Soc. Math. Phys. Eng. Sci.* 380, 20200446. doi:10.1098/rsta.2020.0446
- Gelaro, R., McCarty, W., Suárez, M. J., Todling, R., Molod, A., Takacs, L., et al. (2017). The modern-era retrospective analysis for research and applications, version 2 (MERRA-2). *J. Clim.* 30, 5419–5454. doi:10.1175/JCLI-D-16-0758.1
- Hengl, T., Jesus, J. M., Heuvelink, G. B. M., Gonzalez, M. R., Kilibarda, M., Blagotić, A., et al. (2017). SoilGrids250m: global gridded soil information based on machine learning. *PLOS ONE* 12, e0169748. doi:10.1371/journal.pone.0169748
- Ishizawa, M., Mabuchi, K., Shirai, T., Inoue, M., Morino, I., Uchino, O., et al. (2016). Inter-annual variability of summertime CO₂ exchange in Northern Eurasia inferred from GOSAT XCO₂. *Environ. Res. Lett.* 11, 105001. doi:10.1088/1748-9326/11/10/105001
- Jensen, K., and McDonald, K. (2019). Surface water microwave product series version 3: a near-real time and 25-year historical global inundated area fraction time series from active and passive microwave remote sensing. *IEEE Geosci. Remote Sens. Lett.* 16, 1402–1406. doi:10.1109/LGRS.2019.2898779
- Koffi, E. N., Bergamaschi, P., Alkama, R., and Cescatti, A. (2020). An observation-constrained assessment of the climate sensitivity and future trajectories of wetland methane emissions. *Sci. Adv.* 6, eaay4444. doi:10.1126/sciadv.aay4444
- Kuhn, M., Lundin, E. J., Giesler, R., Johansson, M., and Karlsson, J. (2018). Emissions from thaw ponds largely offset the carbon sink of northern permafrost wetlands. *Sci. Rep.* 8, 9535. doi:10.1038/s41598-018-27770-x
- Lan, X., Thoning, K. W., and Dlugokencky, E. J. (2022). Global monitoring laboratory - carbon cycle greenhouse gases. Available at: https://gml.noaa.gov/ccgg/trends_ch4/ (Accessed June 7, 2023).
- Liu, L., Zhuang, Q., Oh, Y., Shurpali, N. J., Kim, S., and Poulter, B. (2020). Uncertainty quantification of global net methane emissions from terrestrial ecosystems using a mechanistically based biogeochemistry model. *J. Geophys. Res. Biogeosciences* 125. doi:10.1029/2019JG005428
- Liu, Y., Piao, S., Gasser, T., Ciais, P., Yang, H., Wang, H., et al. (2019). Field-experiment constraints on the enhancement of the terrestrial carbon sink by CO₂ fertilization. *Nat. Geosci.* 12, 809–814. doi:10.1038/s41561-019-0436-1
- Lunt, M. F., Palmer, P. I., Lorente, A., Borsdorff, T., Landgraf, J., Parker, R. J., et al. (2021). Rain-fed pulses of methane from East Africa during 2018–2019 contributed to atmospheric growth rate. *Environ. Res. Lett.* 16, 024021. doi:10.1088/1748-9326/abd8fa
- Nzotungicimpye, C.-M., Zickfeld, K., MacDougall, A. H., Melton, J. R., Treat, C. C., Eby, M., et al. (2021). WETMETH 1.0: a new wetland methane model for implementation in Earth system models. *Geosci. Model Dev.* 14, 6215–6240. doi:10.5194/gmd-14-6215-2021
- Piao, S., Sitch, S., Ciais, P., Friedlingstein, P., Peylin, P., Wang, X., et al. (2013). Evaluation of terrestrial carbon cycle models for their response to climate variability and to CO₂ trends. *Glob. Change Biol.* 19, 2117–2132. doi:10.1111/gcb.12187
- Rößger, N., Sachs, T., Wille, C., Boike, J., and Kutzbach, L. (2022). Seasonal increase of methane emissions linked to warming in Siberian tundra. *Nat. Clim. Change* 12, 1031–1036. doi:10.1038/s41558-022-01512-4
- Salmon, E., Jégou, F., Guenet, B., Jourdain, L., Qiu, C., Bastrov, V., et al. (2022). Assessing methane emissions for northern peatlands in ORCHIDEE-PEAT revision 7020. *Geosci. Model Dev.* 15, 2813–2838. doi:10.5194/gmd-15-2813-2022
- Saunio, M., Stavert, A. R., Poulter, B., Bousquet, P., Canadell, J. G., Jackson, R. B., et al. (2020). The global methane budget 2000–2017. *Earth Syst. Sci. Data* 12, 1561–1623. doi:10.5194/essd-12-1561-2020
- Scholes, R. J., Eric, B. D. C., Collatz, F. G. H., Meeson, B. W., Los, S. O., and Landis, D. R. (2011). *Data from: ISLSCP II global gridded soil characteristics*. USA: ORNL DAAC Oak Ridge Tenn. doi:10.3334/ORNLDAAC/1004
- Shaw, J. T., Allen, G., Barker, P., Pitt, J. R., Pasternak, D., Bauguitte, S. J.-B., et al. (2022). Large methane emission fluxes observed from tropical wetlands in Zambia. *Glob. Biogeochem. Cycles* 36, e2021GB007261. doi:10.1029/2021GB007261
- Spitters, C. J. T., Toussaint, H. A. J. M., and Goudriaan, J. (1986). Separating the diffuse and direct component of global radiation and its implications for modeling canopy photosynthesis Part I. Components of incoming radiation. *Agric. For. Meteorol.* 38, 217–229. doi:10.1016/0168-1923(86)90060-2
- Staniaszek, Z., Griffiths, P. T., Folberth, G. A., O'Connor, F. M., Abraham, N. L., and Archibald, A. T. (2022). The role of future anthropogenic methane emissions in air quality and climate. *Npj Clim. Atmos. Sci.* 5, 21–28. doi:10.1038/s41612-022-00247-5
- Turner, A. J., Frankenberg, C., and Kort, E. A. (2019). Interpreting contemporary trends in atmospheric methane. *Proc. Natl. Acad. Sci.* 116, 2805–2813. doi:10.1073/pnas.1814297116
- Walter, B. P., and Heimann, M. (2000). A process-based, climate-sensitive model to derive methane emissions from natural wetlands: application to five wetland sites, sensitivity to model parameters, and climate. *Glob. Biogeochem. Cycles* 14, 745–765. doi:10.1029/1999GB001204

- Wania, R., Ross, I., and Prentice, I. C. (2010). Implementation and evaluation of a new methane model within a dynamic global vegetation model: LPJ-WHyMe v1.3.1. *Geosci. Model Dev.* 3, 565–584. doi:10.5194/gmd-3-565-2010
- Xi, Y., Peng, S., Ducharme, A., Ciais, P., Gumbrecht, T., Jimenez, C., et al. (2022). Gridded maps of wetlands dynamics over mid-low latitudes for 1980–2020 based on TOPMODEL. *Sci. Data* 9, 347. doi:10.1038/s41597-022-01460-w
- Yuan, F., Wang, Y., Ricciuto, D. M., Shi, X., Yuan, F., Hanson, P. J., et al. (2021). An integrative model for soil biogeochemistry and methane processes. II: warming and elevated CO₂ effects on peatland CH₄ emissions. *J. Geophys. Res. Biogeosciences* 126, e2020JG005963. doi:10.1029/2020JG005963
- Yue, X., and Unger, N. (2015). The Yale Interactive terrestrial Biosphere model version 1.0: description, evaluation and implementation into NASA GISS ModelE2. *Geosci. Model Dev.* 8, 2399–2417. doi:10.5194/gmd-8-2399-2015
- Yue, X., Unger, N., and Zheng, Y. (2015). Distinguishing the drivers of trends in land carbon fluxes and plant volatile emissions over the past 3 decades. *Atmos. Chem. Phys.* 15, 11931–11948. doi:10.5194/acp-15-11931-2015
- Zhang, Y., Jacob, D. J., Lu, X., Maasakkers, J. D., Scarpelli, T. R., Sheng, J.-X., et al. (2021a). Attribution of the accelerating increase in atmospheric methane during 2010–2018 by inverse analysis of GOSAT observations. *Atmos. Chem. Phys.* 21, 3643–3666. doi:10.5194/acp-21-3643-2021
- Zhang, Z., Fluet-Chouinard, E., Jensen, K., McDonald, K., Hugelius, G., Gumbrecht, T., et al. (2021b). Development of the global dataset of wetland area and dynamics for methane modeling (WAD2M). *Earth Syst. Sci. Data* 13, 2001–2023. doi:10.5194/essd-13-2001-2021
- Zhang, Z., Poulter, B., Feldman, A. F., Ying, Q., Ciais, P., Peng, S., et al. (2023). Recent intensification of wetland methane feedback. *Nat. Clim. Change* 13, 430–433. doi:10.1038/s41558-023-01629-0
- Zhang, Z., Zimmermann, N. E., Stenke, A., Li, X., Hodson, E. L., Zhu, G., et al. (2017). Emerging role of wetland methane emissions in driving 21st century climate change. *Proc. Natl. Acad. Sci.* 114, 9647–9652. doi:10.1073/pnas.1618765114
- Zhu, Q., Liu, J., Peng, C., Chen, H., Fang, X., Jiang, H., et al. (2014). Modelling methane emissions from natural wetlands by development and application of the TRIPLEX-GHG model. *Geosci. Model Dev.* 7, 981–999. doi:10.5194/gmd-7-981-2014
- Zhu, Q., Peng, C., Chen, H., Fang, X., Liu, J., Jiang, H., et al. (2015). Estimating global natural wetland methane emissions using process modelling: spatio-temporal patterns and contributions to atmospheric methane fluctuations. *Glob. Ecol. Biogeogr.* 24, 959–972. doi:10.1111/geb.12307
- Zou, J., Ziegler, A. D., Chen, D., McNicol, G., Ciais, P., Jiang, X., et al. (2022). Rewetting global wetlands effectively reduces major greenhouse gas emissions. *Nat. Geosci.* 15, 627–632. doi:10.1038/s41561-022-00989-0